



SEISMIC RELIABILITY ANALYSIS OF 3D NON-LINEAR BASE-ISOLATED STRUCTURES WITH FPS

P. Castaldo⁽¹⁾, B. Palazzo⁽²⁾, P. Della Vecchia⁽³⁾

⁽¹⁾ Research Assistant, Dept. of Civil Engineering, University of Salerno, E-mail: pcastaldo@unisa.it

⁽²⁾ Professor, Dept. of Civil Engineering, University of Salerno, E-mail: palazzo@unisa.it

⁽³⁾ Graduate Student, Dept. of Civil Engineering, University of Salerno, E-mail: dellavecchiapasquale@gmail.com

Abstract

The aim of the study consists in evaluating the seismic reliability and life-cycle costs of a reinforced concrete 3D system isolated by FPS bearings with different isolated periods in order to evaluate the potential benefits provided by increasing values of the isolation degree. Assuming the elastic response pseudo-acceleration related to each isolated period and the coefficient of friction as random variables relevant to the problem characterized by appropriate probability density functions, the Latin Hypercube Sampling method has been adopted as random sampling technique in order to define the input data. Several 3D non-linear dynamic analyses have been performed considering both the vertical and horizontal components of each seismic excitation in order to evaluate the system performance. Thus, bivariate structural performance curves for each story of the superstructure and for the substructure as well as seismic reliability-based design (SRBD) curves for the isolation level have been defined for the different values of the isolation degree. Finally, the life-cycle cost analysis of the isolated system with different curvature radius of the FP bearings has been accomplished taking into account both the initial costs and the expected loss costs, due to future earthquakes, of the overall system during its design life (50 years) in order to evaluate the influence of the isolation degree on both the seismic performance and the total costs.

Keywords: isolation degree; life-cycle cost analysis; seismic reliability; FP bearings; joint PDF.

1. Introduction

Seismic isolation through friction pendulum system (FPS) devices represents a widely used and effective technique for the seismic protection of buildings, bridges and industrial structures [1],[2] and many advantages can be achieved by employing such kind of frictional isolators [3]-[5]. Over the years, several research works have been focused on probabilistic analyses, structural reliability methods and reliability-based analysis [6]-[8] as well as Monte Carlo simulations aimed at evaluating reliability of base-isolated systems have been performed by Fan and Ahmadi [9] and Su and Ahmadi [10]. Moreover, several studies have also dealt with (i) reliability analysis and reliability-based optimization of base-isolated systems including uncertainties such as isolation device properties and ground motion characteristics [11], (ii) influence of the isolator properties on the seismic performance of base-isolated buildings adopting an equivalent two-degree-of-freedom model [12] as well as optimal friction coefficient values for different soil conditions [13], (iii) seismic reliability analyses of a base-isolated RC 3D system by accounting for the randomness of both the isolator properties and earthquake main characteristics [14]-[17] in order to define a reliability criterion to assist the design of the isolator dimensions in plan by considering the three-dimensional effects and correlations between the plane response parameters. With reference to the management of new and existing civil structures in earthquake engineering, a widely recognized assessment tool for the system performance estimation, capable to take also into account the potential damages due to future earthquakes, is based on the cost-effectiveness criterion as discussed by Ang and Lee [18]-[20]. In this context, this work aims to further advance the study of Castaldo et al. [15] by evaluating the life-cycle costs of a RC 3D system isolated by FPS bearings with different isolated periods in order to evaluate the potential benefits provided for increasing values of the isolation degree [21],[22]. In particular, assuming the elastic response pseudo-acceleration related to each isolated period and the coefficient of friction as the random variables relevant to the problem, characterized by appropriate probability density functions (PDFs) according to [23] and [24]-[26], respectively, the Latin Hypercube Sampling method (LHS) [27] has been adopted as random sampling technique in order to define the input data and perform 3D non-linear dynamic analyses. For each dynamic analysis, the three dimensional components of each seismic event and the nonlinear behaviour of the superstructure, designed in full compliance with NTC08 [23], have been considered. Thus, bivariate structural performance (SP) curves for each story of the superstructure and for the substructure as well as seismic reliability-based design (SRBD) abacuses for the isolation level have been defined for the different values of the isolation degree. Finally, the life-cycle cost analysis (LCCA) [28]-[30] for the different configurations of the isolated system with various curvature radius of the FP bearings has been accomplished taking into account both the initial costs and the expected loss costs, due to future earthquakes, of the overall system during its design life (50 years) in order to evaluate the influence of the isolation degree on both the seismic performance and the total costs.

2. Life-cycle cost analysis (LCCA)

Within the life-cycle cost analysis (LCCA) of a base-isolated (BI) structure, the cost-effectiveness criterion is based on the computation of the costs related to both the protection system (including substructure, superstructure and isolation devices) and potential losses caused by future earthquakes within its design life and, as suggested by [31],[32], may be useful to achieve an optimization of the design variables. The total expected life-cycle cost [18],[33] of a BI structure is assumed to be the sum between the initial construction cost C_{IN} and the present worth of the lifetime limit state dependent cost C_{LS} as expressed in Eq. (1):

$$C_{TOT} = C_{IN}(s) + C_{LS}(t, s) \quad (1)$$

where t is the design-life time period of the structure, s is the design vector composed of the structural parameters influencing the performance of the structural system (i.e., isolation degree I_d), $C_{IN}(s)$ is the initial construction cost and $C_{LS}(t, s)$ is the limit state dependent cost, also defined as the cumulative damage cost in present worth, including direct damage cost and indirect loss under all earthquakes that could occur over the life of the structure.

The initial construction cost $C_{IN}(s)$ takes into account for (i) initial and regular maintenance cost of the isolation devices and (ii) initial system (superstructure and substructure) construction cost. The initial cost of the

isolation devices is defined on the basis of the radius in plan r of the concave surface of the FPS bearings required to respect the target reliability level (or the target exceeding probability related to the collapse state, i.e., equal to $P_f = 1.5 \cdot 10^{-3}$ for a design life of 50 years) as obtained from the SP_{isolator} curves derived within the seismic reliability analysis. The regular maintenance replacement cost of the isolation devices is the cost of their replacement after 10 years service life [23]. The initial system (substructure and superstructure) construction cost is assumed to be proportional to the initial FP bearings cost being the influence of the isolation system cost on the construction cost of an ordinary building equal to about 5-10% [34].

The limit state dependent cost $C_{LS}(t, \mathbf{s})$ takes into account (i) special maintenance cost of the isolation devices $C_{LS,d}$ and (ii) limit state cost for the i th limit state of the structure (substructure and superstructure) $C_{LS,s}$. The special maintenance cost of isolation devices is the present worth of the cost required to replace the devices if the maximum allowable isolator displacement (radius in plan r) will be reached or exceeded due to the occurrence of the significant earthquakes considered. The limit state cost for the i th limit state on the substructure and superstructure is given by potential direct damage cost and indirect loss under the significant earthquake events that can occur during the design life of the system. As for the limit states, the performance based-design framework, defined in SEAOC [35], focused the attention on four structural performance levels related to four damage levels on a structure, or limit states “ $LS1$ ”, “ $LS2$ ”, “ $LS3$ ”, “ $LS4$ ”, corresponding respectively to “fully operational”, “operational”, “life safety” and “collapse prevention”. In Table 1, the cost categories with the corresponding calculation formulas and the basic costs, described in [29], are reported. Each one of these cost items is based on a damage index or expected rate data according to FEMA-227 [36] and ATC-13 [37]. In Table 2, regarding the abovementioned four limit states, the calculation indices and rates useful to define the limit state dependent costs of Table 1, defined according to FEMA-227 and ATC-13 provisions, are reported. Therefore, the limit state cost for the i th limit state on the structure (superstructure and substructure) $C_{LS,s}^i$ can be expressed as follows in Eq. (2):

$$C_{LS,s}^i = C_1^i + C_2^i + C_3^i + C_4^i + C_5^i + C_6^i + C_7^i \quad (2)$$

where the value of each term on the right side is calculated as the product between the corresponding value reported in Table 1 and the relative indices and rates given in Table 2. The limit state dependent cost function of the overall system, considering (i) N damage states and assuming that (ii) the earthquake occurrence is based on a Poisson process model and (iii) the building is immediately fully restored to its original condition after each damage, has been assumed as in [29],[33], considering the following expressions in Eq. (3)-(5):

$$C_{LS}(t, \mathbf{s}) = \frac{\nu}{\lambda} (1 - e^{-\lambda t}) \sum_{i=1}^N C_{LS,Sum}^i P_i \quad (3)$$

where

$$P_i = P(\Delta > \Delta_i) - P(\Delta > \Delta_{i+1}) \quad (4)$$

and

$$P(\Delta > \Delta_i) = -\frac{1}{\nu t} \ln[1 - P_{t=1}(\Delta > \Delta_i)] \quad (5)$$

where ν is the annual occurrence rate of the significant earthquake [29], modelled by a Poisson process, t is the design-life time period of the structure, $(1 - e^{-\lambda t})/\lambda$ gives the present worth of the cumulative damage cost, λ is the annual monetary discount rate, considered equal to 5% [29],[30], P_i is the probability of the i th damage state being violated given the earthquake occurrence, Δ_i and Δ_{i+1} are the lower and upper bounds of the i th limit state, $P(\Delta > \Delta_i)$ and $P_{t=1}(\Delta > \Delta_i)$ are the lifetime and annual exceeding probability of the i th limit state expressed in terms of the bivariate maximum interstory drift $\Delta_i = \delta_i$, as defined in the following sections. The limit state special maintenance cost of isolation devices, $C_{LS,d}$, is the cost necessary to keep the original capability of the devices and can be expressed through Eq. (3) considering the only limit state, $i = 1$, for which the displacement demand results to be equal to the design displacement of the FPS isolators, $\Delta = u = r$, within the FPS service-life $t = 10$ years.

Table 1 – Limit state dependent cost calculation formula [29]

Cost Category	Calculation formula	Basic cost	
C_1 - Damage	Replacement cost x floor area x mean damage index	1500	MU / m ²
C_2 - Loss of content	Unit contents cost x floor area x mean damage index	500	MU / m ²
C_3 - Rental	Rental rate x gross leasable area x loss of function	10	MU / month / m ²
C_4 - Income	Rental rate x gross leasable area x down time	2000	MU / year / m ²
C_5 - Minor Injury	Minor injury cost per person x floor area x occupancy rate x expected minor injury rate	2000	MU / person
C_6 - Serious Injury	Serious injury cost per person x floor area x occupancy rate x expected serious injury rate	2.00E+04	MU / person
C_7 - Human death	Human fatality cost per person x floor area x occupancy rate x expected death rate	2.80E+06	MU / person
Occupancy rate 2 person / 100 m ²			

Table 2 – Limit states, interstory drift index, damage index, minor injury, serious injury and death rate, average loss of function and down time [15],[36]-[37]

Limit State	BI structure Interstory Drift Index (%)	FEMA 227				ATC 13	
		Mean damage index (%)	Expected minor injury rate	Expected serious injury rate	Expected death rate	Loss of function (%)	Down time (%)
$LS1$	0 < IDI < 0.1 (FEMA 274) 0 < IDI < 0.2 (NTC08)	5	0.0003	0.00004	0.00001	3.33	3.33
$LS2$	0.1 < IDI < 0.2 (FEMA 274) 0.2 < IDI < 0.4 (NTC08)	20	0.003	0.0004	0.0001	12.4	12.4
$LS3$	0.2 < IDI < 0.5 (FEMA 274) 0.4 < IDI < 1.0 (NTC08)	45	0.03	0.004	0.001	34.8	34.8
$LS4$	IDI > 0.7 (FEMA 274) IDI > 1.3 (NTC08)	100	0.4	0.4	0.2	100	100

3. Structural models and uncertainties for the seismic reliability analysis

As also discussed in [15], four structural performance objective (PO) levels according to [35],[38]-[41] are coupled with appropriate reliability indices β , or exceeding probability of the limit states, during the design life of the structure [42]. The considered limit states with the reliability indices as well as the maximum interstory drift limits related to a fixed-base (FB) structure and the maximum interstory drift limits, reduced according to both American [43] and Italian seismic code [23] provisions, for base-isolated (BI) systems have been reported in Fig. 1, which illustrates the performance objective (PO) curves for fixed-base and base-isolated systems. The assessment of the seismic reliability of a base-isolated structure is carried out by comparing the structural capacity of the building, structural performance (SP) curves, to the PO curves.

As for the structural system, four different models of a 3D RC base-isolated building with a design life of 50 years have been considered in order to evaluate the influence of the isolation degree $I_d = (T_{is} / T_{fb})$ [21],[22],

on both the seismic reliability and life-cycle costs of the overall system. The four-story symmetric reinforced concrete 3D frame building, analysed in similar studies [15],[44], has been adopted in this work as benchmark building model. The superstructure and substructure, disconnected by the isolation level, are, respectively, composed of three (4th, 3rd, 2nd stories) and one (1st story) levels. The beams rectangular cross sections are the same in all stories and all frames, as well as all the superstructure and substructure columns have the same square cross section, respectively. The plan dimensions of the structure are 8.0 x 16.0 m with slabs having a depth of 0.40 m; the interstory height of the superstructure is 3.5 m; superstructure column section dimensions are 0.70 x 0.70 m, respectively; beam section dimensions are 0.40 x 0.70 m for each floor level. Story masses is amounted to 100 tons for each story, leading to a total seismic weight of the structure $W_s = 512.0$ tons. The substructure is composed of six columns having 0.80 x 0.80 m section dimension with a height equal to 3.0 m. The four different base-isolated structural models (SM) have been designed by employing friction pendulum isolators with different radius of curvature R and considering a common low value of the sliding coefficient of friction $\mu = 3\%$: SM_1 ($R = 1.5$ m, $I_d = 4.5$), SM_2 ($R = 2.0$ m, $I_d = 5.3$), SM_3 ($R = 3.0$ m, $I_d = 6.4$), SM_4 ($R = 4.0$ m, $I_d = 7.4$). The first natural period of the fixed-base structure results being $T_{fb} = 0.58$ s, the period of the base-isolated model ranges from $2.58 \text{ s} < T_{is} < 4.01$ s, leading to values of the isolation degree I_d higher than 3 for all the configurations, as recommended in the Italian seismic code provisions [23] and in [45].

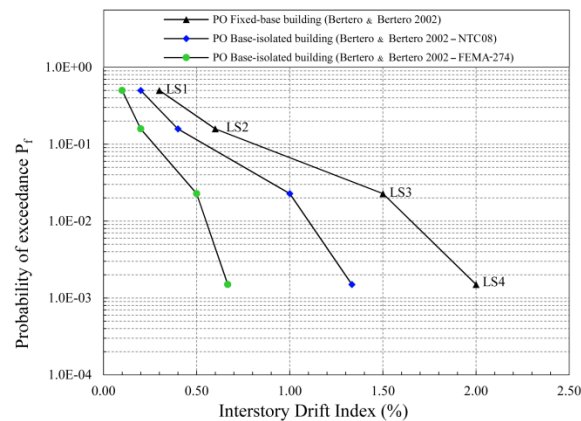


Fig. 1– Exceeding probability (in 50 years) corresponding to the performance limit states in the “performance space”

The different structural models have been designed according to the Italian earthquake design requirements for base-isolated structures [23], (geographic coordinates 41°58'25'' N, 13°24'00'' E, Italy), soil type B. The reinforcement bars of the structural members have been designed through the response spectrum analysis by employing the NTC08 response spectrum for an earthquake event with 475 years return period (corresponding to life limit state) and a reduction factor $q = 1.5$ [23]. Moreover, the non-linear behaviour of the isolation level has been taken into account, considering an equivalent linear behaviour [22],[45] of the friction isolators estimating the effective stiffness K_{eff} , the corresponding effective period T_{eff} and effective damping ζ_{eff} . The superstructure results to be characterised by an overstrength factor higher than 1.2 in both directions. The life safety design is in compliance also with all the recommendations provided in [35],[43]. With reference to an earthquake event with 475 years return period corresponding to operational limit state, the stiffness of the frames is adequate to respect the more restrictive plane and spatial requirements for base-isolated systems according to both [23] and [43] at each story.

Designed the reinforcement bars of the structural members, a FEM model, Fig. 2, has been defined in SAP2000 [46] with the aim to perform 3D non-linear dynamic analyses considering the non-linear behavior of the overall system (superstructure, substructure and isolation level). Each floor has been modelled as diaphragm and assumed to be rigid in its own plane. As for the non-linear behavior of the isolation level, the FPS isolators have been modelled taking into account the velocity dependence of the coefficient of friction as described in [47],[48]. For a such kind of isolators, the force relative to a displaced position is defined by Eq. (6):

$$F = \mu W sgn(\dot{u}) + \frac{W}{R} u \quad (6)$$

in which, sgn denotes the signum function of the sliding velocity u . In SAP2000 [46], the force–deformation behavior of the FP isolator has been modelled through a non-linear hysteretic rule such as a bilinear model [22] without considering any bi-axial interaction in the behavior of the FP system within the hypotheses of the models and parameters adopted. Three parameters, the characteristic strength Q_d given by $Q_d = \mu W$, the post-elastic stiffness determined as $K_2 = W/R$ and the elastic stiffness K_1 , characterize the bi-linear hysteresis loop of the non-linear force deformation behavior of the FP bearing. The dependence of the friction μ on sliding velocity is expressed as [24]-[26], Eq. (7):

$$\mu = f_{max} - (f_{max} - f_{min})exp(-au) \quad (7)$$

where f_{max} and f_{min} are the sliding coefficients of friction at large velocity and nearly zero sliding velocity respectively. The rate parameter “ a ” equal to 50 sec/m and a ratio between f_{max} and f_{min} equal to 3 have been selected according to the experimental data [24]. As for the non-linear mechanical behavior of the RC structural members implemented in SAP2000, beam and column elements are modelled as non-linear frame elements with lumped plasticity. For the column hinges the interaction between the axial force and the bending moments (P - M_y - M_x) has been taken into account, while the bending moments (M_y - M_x) interaction has been considered for the beams hinges.

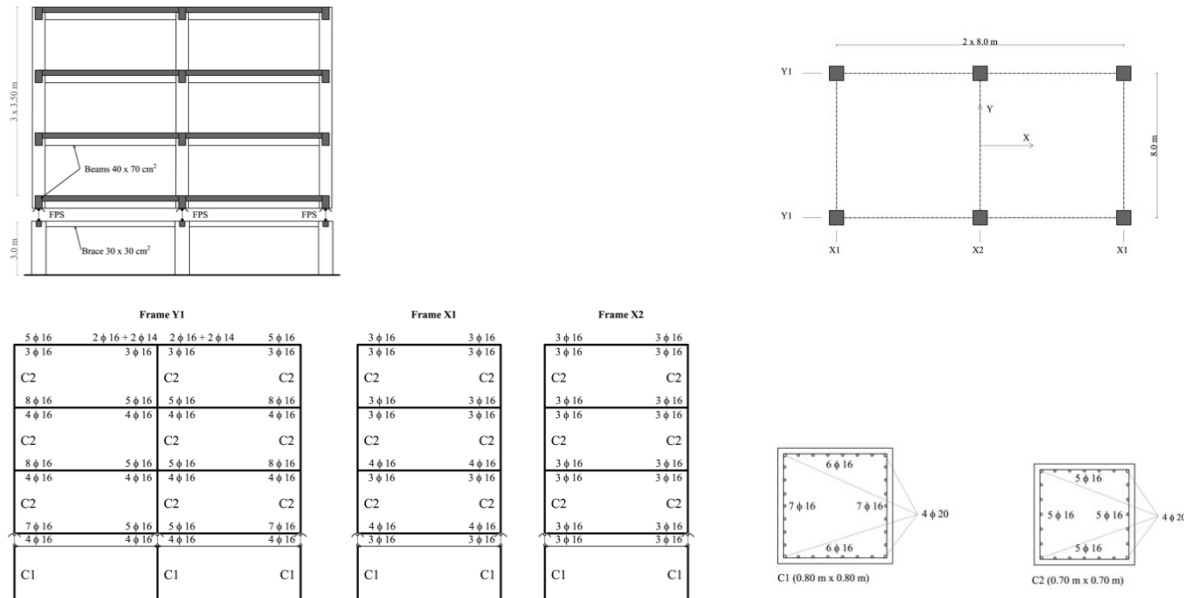


Fig. 2 – Four-story base-isolated benchmark model: front and plan views; beams and columns reinforcement bars

Regarding the uncertainties relevant to the problem, according to [15], the isolator sliding coefficient of friction and the ground motion intensity (i.e., elastic response accelerations at the isolated structural periods with a damping coefficient equal to 2%), are considered as independent random variables.

As for the uncertainty on the sliding friction coefficient, the experimental data developed by [24]-[26] have pointed out that several mechanisms contribute to its variability and can modify its statistical values under dynamic conditions showing a very high uncertainty within the range considered. A uniform probability density function in the range $0.03 < \mu < 0.15$ is assumed to model the coefficient of friction f_{max} as random variable.

The uncertainty of ground motions has been taken into account, according to the probabilistic seismic hazard analysis (PSHA) [49],[50], assuming the intensity measure (IM), $lnS_a(T_{is})[g]$, as a random variable characterized by a Gaussian probability density function (PDF). In this study, the elastic response pseudo-accelerations at the isolated periods of the system, $S_a(T_{is}) [g]$, are assumed as intensity measure according to [51],[52]. With reference to the location (geographic coordinates: 41°58'25'' N, 13°24'00'' E) near L'Aquila site (Italy), design life of 50 years and dimensionless damping coefficient equal to $\xi_{is} = 2\%$, Fig. 3 shows on the

left side the elastic acceleration response spectra with exceeding probabilities equal to 81%, 63%, 10% and 5% provided by Italian seismic code highlighting the values of S_a [g] related to the fundamental periods of the four base-isolated structural models. Four Gaussian PDFs of the $\ln S_a$ [g] random variable, represented in Fig. 3 on the right side, corresponding to the fundamental periods of the four base-isolated structural models have been assumed and the corresponding mean ($E[\ln S_a(T_{is})]$) and COV values have been defined by fitting the above-discussed exceeding probabilities related to the 4 limit states provided by NTC08 [23] for each isolated period. The Latin Hypercube sampling (LHS) method [27] has been used to generate the input data samples of the structural models by sampling 22 values from each PDF and perform the non-linear dynamic analyses. More details about the definition of the input data samples may be found in [15]. Unscaled real records with the three components have been selected from the European Strong-Motion Database [53] by matching the 22 spectral accelerations S_a of the ground motions, regarding each T_{is} , with the values sampled from each PDF of the S_a random variable.

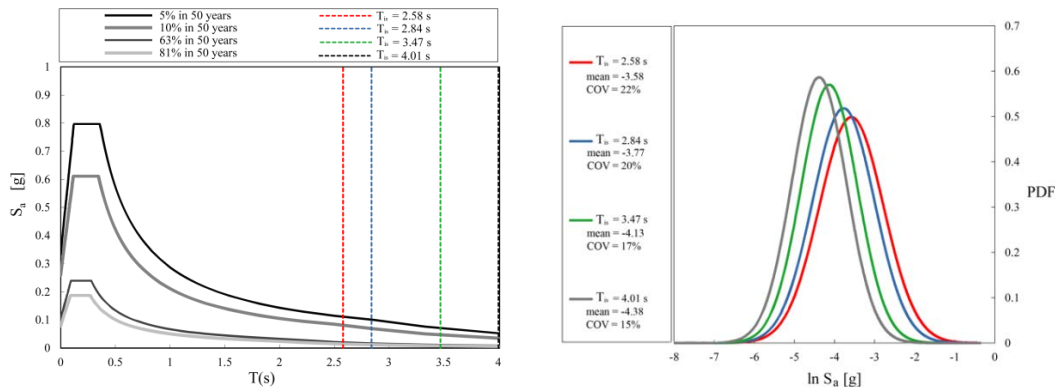


Fig. 3 – Elastic pseudo-acceleration response spectra (in 50 years) ($\xi_{is} = 2\%$, coordinates $41^{\circ}58'25''$ N, $13^{\circ}24'00''$ E, Italy) (left side); PDFs of the seismic intensity measure $\ln S_a$ [g] related to the BI structure periods ($\xi_{is} = 2\%$) (right side)

4. Seismic reliability evaluation

Inelastic response-history analyses have been carried out in SAP2000 on the statistical samples of each structural model. A total number of 484 building samples has been generated for a total number of 1936 non-linear dynamic analyses. As regards the angle column, the absolute maximum interstory drifts, δ_x and δ_y at each level of the superstructure and substructure as well as the absolute maximum isolator relative displacements, u_x and u_y , have been evaluated for each simulation in both directions. The abovementioned response parameters are assumed as earthquake damage parameters (EDPs) according to the performance-based seismic design and to follow a lognormal distribution. Through the maximum likelihood estimation method, the mean and standard deviation of both the absolute maximum interstory drift and the absolute maximum horizontal relative isolator displacement along each direction (x and y directions) have been estimated. As discussed in [15], the three-dimensional effects and correlations between the plane response parameters are not negligible with the consequence that the seismic reliability estimation has to be based on the bivariate exceeding probabilities. It follows that considering the displacements in both directions as dependent and correlated variables and estimating the matrix of correlation coefficients, lognormal bivariate (joint) probability density functions (JPDFs) for the substructure, isolation and each superstructure level have been evaluated (total number of JPDFs equal to 20 being 5 JPDFs for each of the 4 isolation degree I_d). Considering different limit state domains defined on the bi-directional displacements, the seismic reliability of the overall system has been evaluated. In particular, the different limit state functions (performance objectives PO) have been defined in terms of interstory drift (IDI: Interstory Drift Index) [41], reduced according both to FEMA-274 and NTC08 provisions, and isolation relative displacement in order to estimate the exceeding bivariate probabilities P_f . A generic lognormal joint probability density function with generic limit state domains is illustrated in Fig. 4 (left side). Figs 5-6 show the comparison between the SP curves, plotted in logarithmic scale, of the 4th, 3rd and 2nd levels (superstructure) and 1st level (substructure), obtained for the different I_d values, against the PO curves defined as

described in section 3. Seismic reliability for each level of the superstructure and substructure increases (lower exceeding probabilities) with increasing of the isolation degree, as shown in Figs. 5-6, but some limit states are violated due to both the uncertainty characterising the friction coefficient and the vertical components of the seismic excitations. Referring to the more restrictive PO curve defined according to FEMA-274 provisions, the *LS1* is violated for any value of the isolation degree I_d varying in the range of interest. It follows that even with an isolation degree $I_d = 7.4$, (radius of curvature $R = 4.0$ m), concrete cracks (corresponding to slight damage state, *LS1*) at the roof level elements probably occur. Adopting an isolation degree $I_d \geq 6.4$ ($R \geq 3.0$ m) the damage on secondary elements (corresponding to moderate damage state, *LS2*) may be prevented. Referring to the PO curve defined according to NTC08 provisions, no damage should be expected even for the lowest isolation degree I_d considered. Referring to the PO curve defined according to FEMA-274 provisions, the SP curves of the first two levels of the superstructure related to lower values of the isolation degree $I_d = 4.5$ and $I_d = 5.3$, ($R = 1.5$ m and $R = 2.0$ m respectively), plenty exceed the first two limit state *LS1* and *LS2*. Neither adopting $I_d = 7.4$ ($R = 4.0$ m), damage on the secondary elements can be prevented. With reference to the PO curve defined according to NTC08 provisions, the *LS1* is reached for the lowest isolation degree $I_d = 4.5$ ($R = 1.5$ m). The results related to the isolation degree $I_d = 4.5$ ($R = 1.5$ m) are consistent with the results obtained in [15], in which the behaviour of the superstructure is considered linear, due to the value of the overstrength factor. The plan dimension of the isolators (i.e. radius in plan r of the concave surface) can be designed from the (bivariate) structural performance curves of the isolation level, (SP_{isolator}) depicted in Fig. 4 (right side), as also proposed in [15], with the aim to respect an expected reliability level.

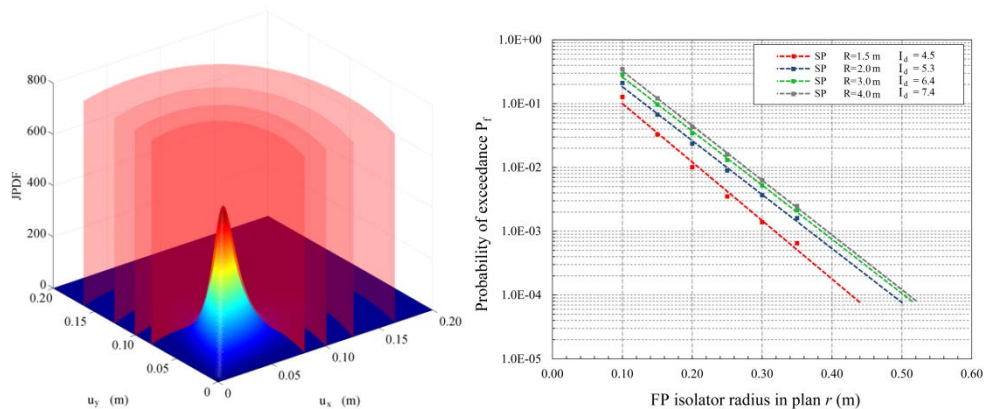


Fig. 4 – Generic lognormal bivariate (joint) probability density function with generic cylindrical limit state domains (left side); Exponential regression curves related to the exceeding bivariate probabilities at the isolation level for different values of the isolation degree I_d (right side)

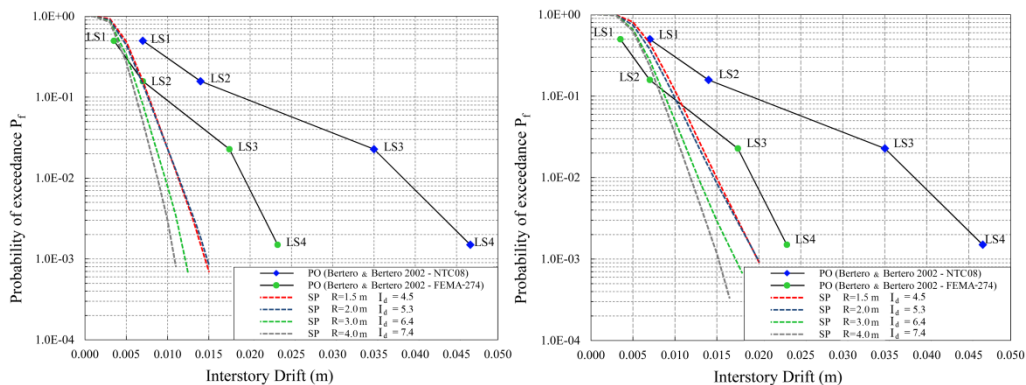


Fig. 5 – Exceeding bivariate probabilities at 4th (left side) and 3rd story (right side) compared to PO curves, for the four different values of the isolation degree I_d

The exponential regression curves of the isolation system related to the exceeding bivariate probabilities for different displacement domains are plotted in Fig. 4 (right side) for the different isolation degrees I_d of interest. Regression curves have been evaluated in the probability range of interest between $1.0E-01$ and $1.0E-03$

for displacements varying from 0.10 m to 0.60 m and show that for a given (bivariate) exceeding probability P_f , a higher value of the radius in plan r is required as the isolation degree I_d increases.

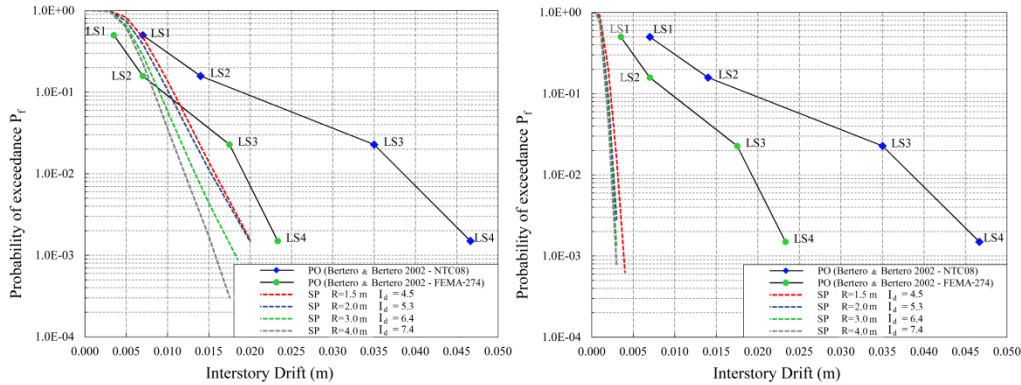


Fig. 6 – Exceeding bivariate probabilities at 2nd (left side) and 1st story (right side) compared to PO curves, for the four different values of the isolation degree I_d

5. Life-cycle cost assessment

The results obtained from the life-cycle cost analysis (LCCA) applied to the four different configurations of the base-isolated system and referred to both FEMA-274 and NTC08 performance objectives are presented and compared. The annual exceedance probabilities of the interstory drifts related to each limit state, $P_{t=1}(\Delta > \Delta_i)$ required in Eq. (6), for each level of the superstructure, substructure and isolation level and for each isolation degree ($I_d = 4.5, I_d = 5.3, I_d = 6.4, I_d = 7.4$), have been obtained starting from the bivariate SP curves illustrated in Fig.s 5-7 and transforming the design-life (50 years) exceeding probabilities into annual exceeding probabilities according to Poisson's model, Eq. (8):

$$P_{t=1} = -\frac{1}{50} \ln(1 - P_f) \quad (8)$$

and, then, substituting $P_{t=1}$ in Eqs. (3)-(4) to calculate the limit state dependent costs for the superstructure and substructure. The limit state dependent cost associated with the isolation devices, special maintenance cost $C_{LS,d}$, has been estimated, for each structural models (SM) configuration, using Eqs. (2)-(3), where t is the service life of the devices, $i = 1$ is the number of limit states considered, $\Delta = r$ is the limit state threshold, taking into account that r is the maximum displacement capability of the devices, designed selecting the radius in in plan of the concave surface for an exceeding probability $P_f = 1.5 \cdot 10^{-3}$ in 50 years ($SP_{isolator}$ curves of Fig. 7). The results obtained from the LCCA for the different isolation degrees and for the both seismic code provisions are shown in Fig. 8. The cost values are based on Eqs. (1)-(5) and calculation formulas of Tables 1-2.

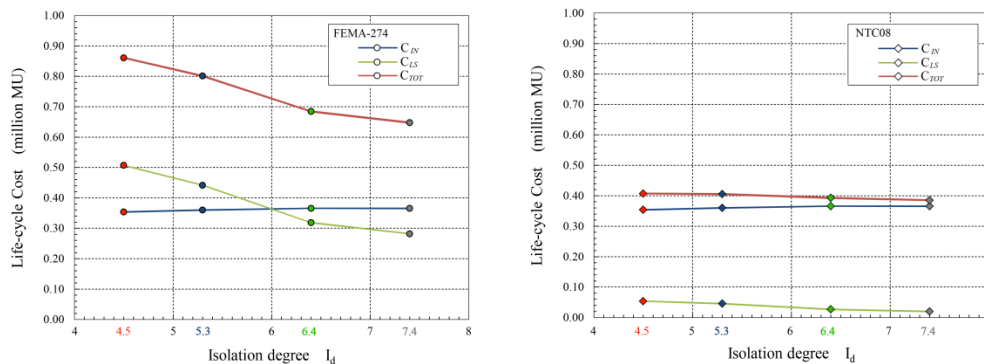


Fig. 8 – Total life-cycle cost of the BI system for different values of the isolation degree I_d respect to PO curves of FEMA-274 (left side) and NTC08 (right side)

The major difference in terms of the total life-cycle cost between the four isolation degrees is given by the limit state dependent cost $C_{LS}(t, s)$. The initial construction costs C_{IN} are independent of the limit state

exceeding probabilities and increase of about 3% from $I_d = 4.5$ to 7.4 because of the initial and regular maintenance costs of the isolation devices. From Fig. 8 (left side), where the limit state dependent costs of superstructure and substructure have been evaluated with reference to the more restrictive FEMA-274 performance objectives, it is possible to note that (i) the limit state dependent cost associated with the low values of the isolation degree highly overcomes the initial construction cost of the building; (ii) an isolation degree $I_d = 7.4$ allows to reduce the expected limit state dependent costs of about 55% if compared to the case with an isolation degree equal to $I_d = 4.5$; (iii) higher values of the isolation degree lead to lower values of the total life-cycle cost demonstrating the effectiveness of the isolation degree for the RC building considered. In Fig. 8 (right side) the limit state dependent costs of the superstructure and substructure have been evaluated with reference to the less restrictive NTC08 performance objectives showing that the limit state dependent cost is a fraction of the construction cost for all the values of I_d due to the very low annual exceeding probabilities of the limit states and that higher values of the isolation degree always lead to lower values of the total life-cycle cost.

6. Conclusions

The influence of the isolation degree on the seismic reliability and life-cycle costs of an ordinary 3D base-isolated RC structure through single-concave FP isolators, considering both earthquake main characteristics and isolator properties as the random variables relevant to the problem, has been evaluated. Several 3D non-linear dynamic analyses have been performed in order to evaluate the system response considering both the vertical and horizontal components of each seismic excitation. Bivariate (joint) probability density functions have been computed and, assuming the limit state domains (performance objectives), the bivariate exceeding probabilities (structural performances) have been estimated in order to compare SP to PO curves. The results from the seismic reliability analysis of the considered system, designed according to NTC08 and FEMA-274, indicate that the seismic reliability of the superstructure and substructure improves as isolation degree I_d increases but some limit states are violated due to both the uncertainty characterising the friction coefficient and the vertical components of the seismic excitations. The structural performance curves of the isolation level, ($SP_{isolator}$) can be used to design the plan dimension of the isolator (i.e., radius in plan r of the concave surface) in order to respect reliability levels depending on the isolation degree. In particular, an exceeding probability of $P_f = 1.5 \cdot 10^{-3}$ (related to the collapse limit state, reliability index $\beta = 3$ in 50 years) is achievable, for $I_d = 4.5$ ($R = 1.5$ m), with a radius in plan $r = 0.3$ m; whereas in the case of $I_d = 7.4$ ($R = 4.0$ m), the same reliability level is achieved with a higher value of r equal to about 0.40 m. The seismic reliability-based design (SRBD) abacuses, proposed in this study, can be used to design the FP bearing devices, having a radius of curvature R ranging from 1.5 m to 4.0 m, employed to seismically isolate regular buildings located in an area characterised by a seismic hazard similar to that considered. Finally, from the results of the life-cycle cost analysis, it is possible to note that (i) the initial cost of the four base-isolated models is similar (about 3% variation); (ii) the major difference in terms of total life-cycle cost between the four isolation degrees is given by the limit state dependent cost especially regarding the more restrictive FEMA-274 performance objectives; (iii) higher values of the isolation degree lead to lower values of the total life-cycle cost demonstrating the effectiveness of the isolation degree for the RC building considered.

7. References

- [1] Christopoulos C, Filiatrault A (2006): Principles of Passive Supplemental Damping and Seismic Isolation. *IUSS Press*: Pavia, Italy.
- [2] Zayas VA, Low SS, Mahin SA (1990): A simple pendulum technique for achieving seismic isolation. *Earthquake Spectra*; **6**, 317–33.
- [3] Jangid RS (2000): Optimum frictional elements in sliding isolation systems. *Computers and Structures*; **76**, 651–661.
- [4] Chen Y, Ahmadi G (1992): Stochastic earthquake response of secondary systems in base-isolated structures. *Earthquake Engineering and Structural Dynamics*; **21**, 1039–57.
- [5] Chen Y, Ahmadi G (1992): Wind effects on base-isolated structures. *J of Engineering Mechanics ASCE*; **118**, 1708–27.
- [6] Lin YK, Cai GQ (1995): Probabilistic structural dynamics—Advanced theory and applications. NY: *McGraw-Hill*.

- [7] Chen J, Liu W, Peng Y, Li J (2007): Stochastic seismic response and reliability analysis of base-isolated structures. *Journal of Earthquake Engineering*; **11**, 903-924.
- [8] Cornell CA, Krawinkler H (2000): Progress and challenges in seismic performance assessment. *PEERCenter News*; **4**(1), 1-3.
- [9] Fan FG, Ahmadi G (1990): Random response analysis of frictional base isolation system. *Journal of Engineering Mechanics*; **116**(9), 1881–901.
- [10] Su L, Ahmadi G (1988): Response of frictional base isolation systems to horizontal–vertical random earthquake excitations. *Probabilistic Engineering Mechanics*; **3**(1), 12–21.
- [11] Alhan C, Gavin HP (2005): Reliability of base isolation for the protection of critical equipment from earthquake hazards. *Engineering Structures*; **27**, 1435-1449.
- [12] Castaldo P, Tubaldi E (2015): Influence of fps bearing properties on the seismic performance of base-isolated structures. *Earthquake Engineering and Structural Dynamics*.
- [13] Castaldo P, Ripani M (2016): Optimal design of friction pendulum system properties for isolated structures considering different soil conditions, *Soil Dynamics and Earthquake Engineering*, 90:74–87, DOI: 10.1016/j.soildyn.2016.08.025.
- [14] Palazzo B, Castaldo P, Della Vecchia P (2014): Seismic reliability of base-isolated structures with friction pendulum isolators (FPS). *2nd European Conference on Earthquake Engineering and Seismology*, Istanbul, Turkey.
- [15] Castaldo P, Palazzo B, Della Vecchia P (2015): Seismic reliability of base-isolated structures with friction pendulum bearings. *Eng Struct*; **95**, 80-93.
- [16] Castaldo P, Palazzo B, Della Vecchia P (2016): Life-cycle cost and seismic reliability analysis of 3D systems equipped with FPS for different isolation degrees, *Engineering Structures*, 125;349–363.
- [17] Castaldo P, Amendola G, Palazzo B (2016): Seismic fragility and reliability of structures isolated by friction pendulum devices: Seismic reliability-based design (SRBD), *Earthquake Engineering and Structural Dynamics*, DOI: 10.1002/eqe.2798.
- [18] Ang AH-S, Lee J-C (2001): Cost optimal design of RC buildings. *Reliab Eng Syst Saf*; **73**, 233-8.
- [19] Castaldo P, De Iuliis M (2014): Optimal integrated seismic design of structural and viscoelastic bracing-damper systems. *Earthquake Engineering and Structural Dynamics*; **43**(12), 1809–1827.
- [20] Castaldo P (2014): *Integrated Seismic Design of Structure and Control Systems*. Springer International Publishing: New York.
- [21] Palazzo B (1991): Seismic Behavior of base-isolated Buildings. *Proceedings of the International Meeting on earthquake Protection of Buildings, Ancona*.
- [22] Naeim F, Kelly JM (1999): *Design of Seismic Isolated Structures: From Theory to Practice*. John Wiley & Sons, Inc.
- [23] NTC08. Norme tecniche per le costruzioni. Gazzetta Ufficiale del 04.02.08, DM 14.01.08, Ministero delle Infrastrutture.
- [24] Constantinou MC, Whittaker AS, Kalpakidis Y, Fenz DM, Warn GP (2007): Performance of Seismic Isolation Hardware Under Service and Seismic Loading. *Technical Report MCEER-07-0012*.
- [25] Constantinou MC, Mokha A, Reinhorn AM (1990): Teflon Bearings in Base Isolation. II: Modeling. *J. Struct. Eng.*; **116**(2), 455-474.
- [26] Mokha A, Constantinou MC, Reinhorn AM (1990): Teflon Bearings in Base Isolation. I: Testing. *J. Struct. Eng.*; **116**(2), 438-454.
- [27] Mckey MD, Conover WJ, Beckman RJ (1979): A comparison of three methods for selecting values of input variables in the analysis from a computer code. *Technometrics*; **21**, 239-45.
- [28] Wen YK, Kang YJ (2001): Minimum building life-cycle cost design criteria I: methodology. *J Struct Eng*; **127**(3), 330 – 7.
- [29] Mitripoulou ChCh, Lagaros ND, Papadrakakis M (2011): Life-cycle cost assessment of optimally designed reinforced concrete buildings under seismic actions. *Reliability Engineering and Structural Safety*; **96**, 1330 – 1331.

- [30] Shin H, Singh M.P (2014): Minimum failure cost-based energy dissipation system design for buildings in three seismic regions – Part I: Elements of failure cost analysis. *Engineering Structures*; **74**, 266 – 274.
- [31] Esteva L, Díaz-López O, García Pérez J, Sierra G, Ismael E (2002): Life-cycle optimization in the establishment of performance-acceptance parameters for seismic design. *Struct Safety*; **24** (2-4), 187-204.
- [32] Ang AH-S, Leon DD (1997): Determination of optimal target reliabilities for design and upgrading of structures. *Structural Safety*; **19**(1), 91–103.
- [33] Wen YK, Kang YJ (2001). Minimum building life-cycle cost design criteria I: methodology. *J Struct Eng*; **127** (3), 330 – 7.
- [34] Clemente P, Buffarini G (2010): Seismic Isolation and Protection Systems. Base Isolation: design and optimization criteria. *The Journal of the Anti-Seismic Systems International Society (ASSISI)*; vol 1, no 1.
- [35] SEAOC-Vision 2000 Committee. Vision 2000—a framework for performance-based earthquake engineering, vol.1. Sacramento (CA): Structural Engineers Association of California; 1995.
- [36] FEMA-227. A benefit-cost model the seismic rehabilitation of buildings. Washington, DC: Federal Emergency Management Agency, Building Seismic Safety Council; 1992.
- [37] ATC-13. Earthquake damage evaluation data for California. Redwood City, CA: Applied Technology Council; 1985.
- [38] Collins KR, Stojadinovic B (2000): Limit states for performance-based design. *12WCEE*.
- [39] Aoki Y, Ohashi Y, Fujitani H, Saito T, Kanda J, Emoto T, Kohno M (2000): Target seismic performance levels in structural design for buildings. *12WCEE*.
- [40] Saito T, Kanda J, Kani N (1998): Seismic reliability estimate of building structures designed according to the current Japanese design code. *Proceedings of the Structural Engineers World Congress*.
- [41] Bertero RD, Bertero VV (2002): Performance-based seismic engineering: the need for a reliable conceptual comprehensive approach. *Earthquake Engineering and Structural Dynamics*; **31**, 627–652 (DOI: 10.1002/eqe.146).
- [42] CEN – European Committee for Standardization. Eurocode 0: Basis of Structural Design. Final draft. Brussels, 2006.
- [43] Building Seismic Safety Council. NEHRP commentary on the guidelines for the seismic rehabilitation of buildings. Provisions (FEMA-274). Washington, DC, 1997.
- [44] Almazàn JL, De la Llera JC (1993): Physical model for dynamic analysis of structures with FPS isolators. *Earthquake Engineering and Structural Dynamics*; **32**, 1157–1184 (DOI: 10.1002/eqe.266).
- [45] Kilar V, Koren D (2009): Seismic behaviour of asymmetric base isolated structures with various distributions of isolators. *Eng Struct*; **31**, 910-921.
- [46] SAP 2000. Computers and Structures Inc.: Berkley, CA, 2002.
- [47] Nagarajaiah S, Reinhorn AM, Constantinou MC (1991): 3D-Basis: Non Linear Dynamic Analysis of Three-Dimensional Base Isolated Structures: Part II. *Technical Report NCEER-91-0005*.
- [48] Tena-Colunga A, Escamilla-Cruz JL (2007): Torsional amplifications in asymmetric base-isolated structures. *Engineering Structures*, **29**(2), 237-47.
- [49] Cornell CA (1968): Engineering seismic risk analysis. *Bulletin of the Seismological Society of America*; **58**(5), 1583–1606.
- [50] Bazzurro P, Cornell CA (1999): Disaggregation of seismic hazard. *Bulletin of the Seismological Society of America*; **89**, 501–520.
- [51] Shome N, Cornell CA, Bazzurro P, Carballo JE (1998): Earthquake, records, and nonlinear responses. *Earthquake Spectra*; **14** (3), 469-500.
- [52] Luco N, Cornell CA (2007): Structure-specific scalar intensity measures for near-source and ordinary earthquake ground motions. *Earthquake Spectra*; **23** (2), 357-92.
- [53] ESMD <http://www.isesd.hi.is/>